AD-A060 957 NAVAL RESEARCH LAB WASHINGTON D C F/G 20/9
EFFECTS OF ATOMIC STRUCTURE ON THE RADIATION DYNAMICS OF AN OPT--ETC(U)
SEP 78 D DUSTON, J DAVIS, K G WHITNEY

UNCLASSIFIED NRL-MR-3846 NL

| OF |
AD
AD80 957

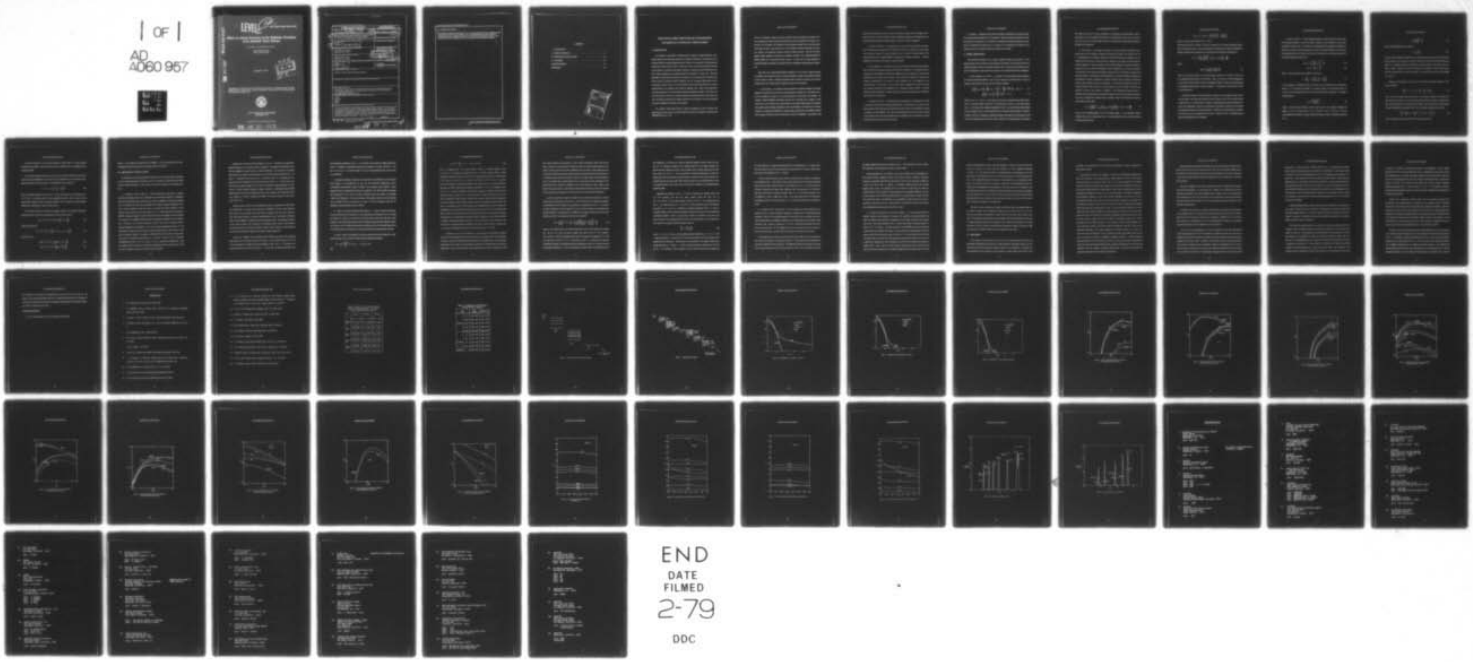

END
DATE
FILMED
2-79
DDC

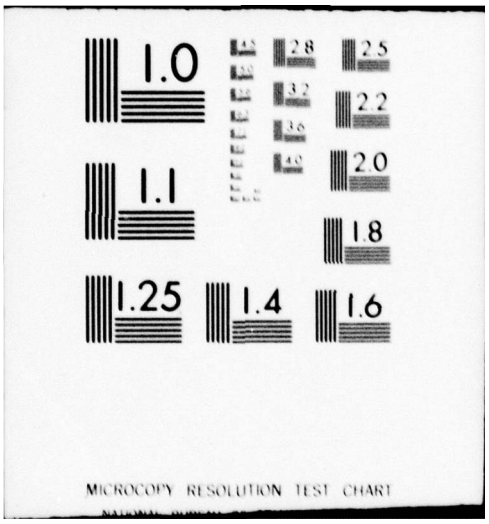
1.0
1.1
1.25
1.4
1.6
2.8
3.2
3.6
4.0
2.5
2.2
2.0
1.8
MICROCOPY RESOLUTION TEST CHART

LEVEL II

NRL Memorandum Report 3846

Effects of Atomic Structure on the Radiation Dynamics of an Optically Thick Plasma

D. DUSTON, J. DAVIS, and K. G. WHITNEY

Plasma Radiation Group
Plasma Physics Division

September 1978

This research was sponsored by the Defense Nuclear Agency under Subtask Code and Title T99QAXLA014, Pulsed Power Advanced Simulation Concepts; Work Unit Code and Title 52, Intermediate BACCARAT.

NAVAL RESEARCH LABORATORY
Washington, D.C.

62704H

SECURITY CLASSIFICATION OF THIS PAGE (When Data Entered)

REPORT DOCUMENTATION PAGE

READ INSTRUCTIONS BEFORE COMPLETING FORM

1. REPORT NUMBER: NRL Memorandum Report 3846
2. GOVT ACCESSION NO.: NRL-MR-3846
3. RECIPIENT'S CATALOG NUMBER
4. TITLE (and Subtitle): EFFECTS OF ATOMIC STRUCTURE ON THE RADIATION DYNAMICS OF AN OPTICALLY THICK PLASMA
5. TYPE OF REPORT & PERIOD COVERED: Memorandum Report
6. PERFORMING ORG. REPORT NUMBER
7. AUTHOR(s): D. Duston,* J. Davis, and K. G. Whitney
8. CONTRACT OR GRANT NUMBER(s)
9. PERFORMING ORGANIZATION NAME AND ADDRESS: Naval Research Laboratory, Washington, D.C. 20375
10. PROGRAM ELEMENT, PROJECT, TASK AREA & WORK UNIT NUMBERS: NRL Problem No. 77H02-26L; DNA Subtask T99QAXLA014
11. CONTROLLING OFFICE NAME AND ADDRESS: Defense Nuclear Agency, Washington, D.C. 20305
12. REPORT DATE: September 1978
13. NUMBER OF PAGES: 59 (61 p.)
14. MONITORING AGENCY NAME & ADDRESS (if different from Controlling Office)
15. SECURITY CLASS. (of this report): Unclassified
15a. DECLASSIFICATION/DOWNGRADING SCHEDULE
16. DISTRIBUTION STATEMENT (of this Report)

Approved for public release; distribution unlimited.

17. DISTRIBUTION STATEMENT (of the abstract entered in Block 20, if different from Report)

18. SUPPLEMENTARY NOTES

This research was sponsored by the Defense Nuclear Agency under Subtask Code and Title T99QAXLA014, Pulsed Power Advanced Simulation Concepts; Work Unit Code and Title, 52, Intermediate BACCARAT.
*NRL-NRC Resident Research Associate

19. KEY WORDS (Continue on reverse side if necessary and identify by block number)

Atomic
Radiation
Opaque
Plasma

20. ABSTRACT (Continue on reverse side if necessary and identify by block number)

A theoretical model has been developed to calculate the effects of atomic level structure on the ionization and radiation dynamics of high-density, high-temperature plasmas. The model solves time-dependent rate equations to calculate the population densities of excited states in a stationary, homogeneous, uniformly-heated volume of plasma. The transport and reabsorption of emitted radiation in an optically thick plasma are modeled phenomenologically with a formalism based on frequency diffusion of the photons. → next page

(Continued)

DD FORM 1 JAN 73 1473 EDITION OF 1 NOV 65 IS OBSOLETE
S/N 0102-014-6601

SECURITY CLASSIFICATION OF THIS PAGE (When Data Entered)

20. ABSTRACT (Continued)

This radiation transport model has been used to obtain preliminary results for comparisons between optically thin and optically thick plasmas. Also, an extensive analysis of several methods for generating electron-ion collisional excitation rates for K-shell ions is presented, as well as a study of the effects of ion-ion collisions on the level populations for relevant plasma conditions.

CONTENTS

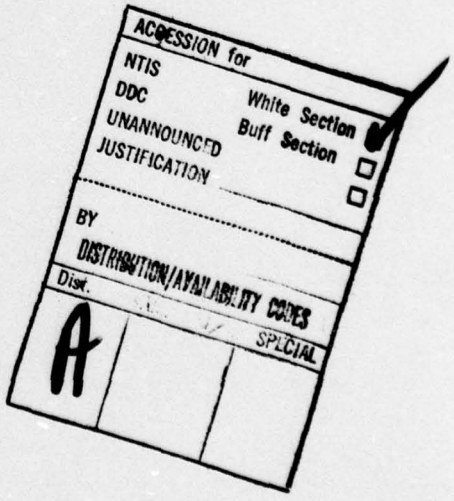

EFFECTS OF ATOMIC STRUCTURE ON THE RADIATION DYNAMICS OF AN OPTICALLY THICK PLASMA

I. INTRODUCTION

The problem of quantitatively characterizing the dynamics of high-temperature, high-density plasmas is one which has received much attention, motivated for the most part, by the continued interest in inertial confinement fusion. However, the complexity of the problems has spawned many efforts which attempt to isolate one or more of the physical processes occurring in these plasmas, in particular, laser-plasma interaction, thermal and non-thermal particle transport, plasma compression, and radiation emission and transport, to name a few. Two basic advantages of approaching the problem in this manner are (i) the opportunity to analyze a specialized model of somewhat reduced complexity, and (ii) the greater sophistication used in describing the smaller but more involved subsystem, both of which ultimately lead to a greater understanding of the subsystem than would be realizable from a larger, more approximate numerical description of the fully-coupled radiation-hydrodynamic problem. This report concerns itself with one facet of the complex processes occurring in transiently heated dense plasmas: the ionization dynamics and radiation emission, and its effects on the overall energetics and resultant diagnostics associated with the plasma.

We consider a small volume element of plasma, homogeneous in total ion density, temperature and material, heated by uniform deposition of energy, and radiating in nearly isotropic

Manuscript submitted June 1, 1978.

manner. We describe, in detail, the atomic ionization state of the plasma, the radiation emission resulting from atomic transitions between states, and the trapping of this radiation as it interacts with the plasma. We characterize these physical processes with a one-dimensional model which involves a self-consistent set of time-dependent equations describing the ionization, radiation, and temperature dynamics during the plasma evolution. We treat a stationary plasma thereby isolating the ionization and radiation calculation from magnetohydrodynamic (MHD) effects due to macroscopic plasma motion. A known rate of energy absorption is assumed throughout the plasma, obviating the need for modeling an energy absorption mechanism.

Since this is not a coupled MHD-radiation calculation, it is our intent to apply the model to problems which dictate the need for detail and flexibility in regard to the physical processes we have chosen to include. Although the possible areas of study are numerous, we list several problems which are currently under investigation as part of our initial effort:

1. Level structure — as a basis for accurate prediction of radiation emission from heated plasmas, the atomic level structure of the ions should play an integral role. The number of levels to be included in a model, is, of course, determined by the physics of the problem. For example, valuable diagnostic information may be lost or distorted due to neglect of some atomic levels, to say nothing of the possible effect on the gross energy balance of the plasma. This model has been designed specifically to allow total flexibility in the selection of the atomic structure. For purposes of comparison, ionization stages, energy levels, and radiation transport may be easily and quickly altered to facilitate our structure investigations. One aspect of this

work will be to determine the error incurred in the radiation emission due to the neglect of certain atomic levels in various materials, thereby establishing standards for completeness with a minimum essential amount of structural detail, to be used in further investigations.

2. *Isoelectronic Sequences* — an important part of the level structure problem is the prediction of transition rates, energy levels, and radiation emission (as a function of a given energy level or groups of levels) in similarly charged ions as a function of nuclear charge. These trends should be used to establish different requirements for adequate ionization — radiation descriptions as one goes from moderate to high-Z materials.

3. *Rate Coefficients* — the validity of an atomic level-structure model depends fundamentally on how well the transitions between these levels are described. It is common practice to employ general prescriptions to calculate rate coefficients that are independent of the individual characteristics of a specific ionic transition. While having the advantage of simplistic and economic implementation, the accuracy of these coefficients may be insufficient for the intended model. The alternative is to treat each transition separately and calculate accurately (but at greater expense) the rate coefficient over a temperature range of interest. A problem presently under investigation is to assess the errors incurred when approximate rate coefficients are introduced into calculations.

4. *Population Inversions* — an interesting and useful application of a detailed atomic model is in the area of X-ray and VUV plasma dynamic lasers. The calculation can be used to investigate energy level pairs which appear promising as inversions when an ionized plasma is allowed to expand, cool and recombine. We expect the knowledge gained from the study of isoelectronic sequence trends in level populations will play a significant part in predicting how the gain from an inversion will scale with atomic number.

5. *Diagnostics* — although a given model may neglect some effects for the sake of simplicity and place specific emphasis on a few processes, it should nevertheless be capable of providing predictions for experiment. For example, the calculated line emission spectra can be compared to experimentally obtained data as a measure of the temperature and density in the plasma as a function of heating conditions and plasma atomic number.

II. MODEL DESCRIPTION

The theoretical description of our model is logically divided into three parts: (1) the plasma heating, thermal conduction, and temperature calculation, (2) the atomic structure and ionization dynamics, and (3) the radiation transport model. The first and third topics are common to all calculations, while the second is particular to the specific plasma under investigation.

A. *Energy Deposition and Transfer* — the details of the basic plasma physics included in our model are described elsewhere[1]; only the basic equations are presented here. The set of equation solved include an electron and ion temperature equation,

$$\frac{\partial}{\partial t}\left(\frac{3}{2} N_e k_B T_e\right) + \frac{\partial E_i}{\partial t} = S_e - \frac{3\kappa_e T_e}{\gamma l_e} - \frac{3M_e}{M_i}\frac{N_e k_B}{\tau_e}\left(T_e - T_i\right) - R \qquad (1)$$

$$\frac{\partial}{\partial t}\left(\frac{3}{2} N_i k_B T_i\right) = \frac{3M_e}{M_i}\frac{N_e k_B}{\tau_e}\left(T_i - T_e\right) \qquad (2)$$

where M_e, M_i, T_e, T_i and N_e, N_i are electron and ion mass, temperature and density respectively, κ_e is electron thermal conductivity[2], k_B is Boltzmann's constant, S_e is the energy source term, τ_e is the electron-ion collisional equipartition time[3], R is a term characterizing radiation loss by the plasma, and E_i is energy expended by the electrons during ionization or excitation processes. The term l_e represents a temperature gradient scale length and is determined in such a way as to realistically model conduction losses to regions of the plasma external to the sphere.

The radiation loss term R, contains contributions corresponding to bremsstrahlung, radiative recombination, and line emission processes and will be defined more fully in the next section. The source term S_e, can model energy deposition at any desired rate or pulse shape; presently a Gaussian rate is being used.

B. *Atomic Physics* — the method of solution of the rate equations is identical for any atomic system; only the number of equations to be solved will change. The model solves a set of time-dependent rate equations containing terms which describe the population and de-population of atomic levels. The equations are integrated in time using an iterative predictor-corrector algorithm to obtain convergence while avoiding "stiffness" by separate treatment of asymptotic rates. The method of calculation of the rate coefficients is, of course, fundamental to the accuracy of our ionization and radiation calculation and it is worthwhile to discuss several methods in detail. The processes presently included in our model are collisional ionization and recombination, radiative recombination, collisional excitation and de-excitation, spontaneous emission, and stimulated emission and absorption. The first three processes have been discussed elsewhere[1], while the last two will be discussed in the next section; the spontaneous emission is given by the Einstein A coefficient[4]. The collisional de-excitation process is obtained from detail balancing of the collisional excitation rate; the latter has been calculated in four ways. For approximate collisional rates, a modified version of Van Regemorter's semiclassical method[5] has been used,

$$X_{ij} = 16 \left(\frac{2\pi}{3M_e} \right)^{1/2} \frac{I_H^2}{(k_B T_e)^{1/2} \Delta E} \exp \left(\frac{-\Delta E}{k_B T_e} \right) f_{ij} \langle \bar{g}_{ij} \rangle \pi a_o^2 \frac{\text{cm}^3}{\text{sec}} \qquad (3)$$

where I_H is the Rydberg energy, ΔE is the transition energy, f_{ij} is the transition oscillator strength, and $\bar{g}_{ij}$ is an average Gaunt factor. In this approximation, Allen's values[6] have been used and parameterized by[7]

$$\langle \bar{g} \rangle = A + (BY + C)\left[\ln\left(\frac{Y+1}{Y}\right) - \frac{0.4}{(Y+1)^2}\right],$$

where A, B, and C are constants, and $Y = \Delta E/T_e$.

When greater accuracy is required, the rates are calculated by the method of distorted waves.[8] We have calculated rates for several hydrogenlike and heliumlike ions along the isoelectronic sequence using the Born approximation as parameterized by Vainshtein and Sobel'man[9],

$$X_{ij} = 10^{-8}\left(\frac{I_H}{\Delta E}\left(\frac{E_i}{E_j}\right)^2\right)^{3/2} \frac{1}{2l_i+1}\,\alpha\,\phi\,(\beta)\,\frac{e^{-\beta}}{\beta+\chi}\,\frac{\text{cm}^3}{\text{sec}}$$

where

$$\phi(\beta) = \begin{cases} \beta^{3/2} & \text{if } \Delta S \neq 0 \\ \sqrt{\beta}\,(\beta+1) & \text{if } \Delta S = 0 \end{cases} \tag{4}$$

Here E is the ionization energy, l is the orbital angular momentum, $\beta = \Delta E/k_B T_e$, and α and χ are parameters characteristic of the transition. Lastly, in the case of Al XIII (hydrogenlike) we have taken several transition rates from Landshoff and Perez[10], which were calculated using a Coulomb-Born approximation (without exchange). A comparison of these methods is made in a following section.

The atomic structure has been developed, at present, for three plasmas, carbon, aluminum, and argon. The carbon and aluminum structure is shown in Fig. 1 while the argon model is depicted in Fig. 2. Excited states are coupled to neighboring ground states by collisional ionization and recombination (above) and collisional and stimulated excitation and de-excitation and spontaneous emission where allowed (below). In addition, the excited states are coupled to each other by the last 5 processes for all ions but Ar XII and Ar XIV. All adjacent ground states are coupled by the first 3 processes.

C. *Radiation Transport* — a phenomenological radiation transport scheme has been added to the existing formalism to extend the predictive capability of the calculations to cases where the plasma is optically thick. The model used is fundamentally one developed by Julienne and Davis[11] and is based on photon escape from the plasma by frequency diffusion into the wings of the broadened line profile. Effective rates for photon scattering by ions and photon escape rates have been calculated and are given by,

$$t_{e(\text{scape})} = \frac{1}{x_1}\left[\frac{dx}{dt}\bigg|_{x=x_1}\right]^{-1}\frac{\bar{L}}{\tau_o\, c} \tag{5}$$

$$t_{s(\text{catter})} = \frac{2}{\sqrt{\pi}}\, x_1\, \frac{\bar{L}}{\tau_o\, c} \tag{6}$$

where τ_o is the optical depth of the plasma[12] at line center,

$$\tau_o = \frac{\pi e^2}{M_e c}\, f_{ij}\, \frac{\bar{L}\, N_i}{\sqrt{\pi}\, \Delta\nu_D}\left[1 - \frac{g_i\, N_j}{g_j\, N_i}\right], \tag{7}$$

x_1 is the frequency (in Doppler widths) at the point in the line profile where the optical depth drops to 1, $\bar{L}$ is the effective path length, c is the speed of light, g is the statistical weight, and N_i and N_j are the population densities of the lower and upper states, respectively. The Doppler width is given by,

$$\Delta\nu_D = \left[\frac{2k_B T_i}{Mc^2}\right]^{1/2}\nu_o \tag{8}$$

where ν_o is the line center frequency and M is the ion mass. For a Doppler broadened line profile, $x_1 = (\ln \tau_o)^{1/2}$, thus, giving $t_e = 2 \ln \tau_o\, \bar{L}/c$ and $t_s = 2(\ln \tau_o)^{1/2}\, \bar{L}/\sqrt{\pi}\, \tau_o c$. We have also extended the calculation to include Voigt line profiles by using an approximate expression for x_1.

$$x_1 \simeq \left(\frac{\tau_o\, a}{\sqrt{\pi}}\right)^{1/2} 0.8 \tag{9}$$

where, the damping parameter a is given by,

$$a = \frac{A_{ij}}{4\,\pi\,\Delta\,\nu_D} \tag{10}$$

Accurate Voigt and Doppler profiles have been computed numerically to test the validity of the above expression, and the results are shown for several lines of aluminum K-shell transitions in Figs. 3-5. A complete tabulated set of results for various temperatures and densities is given in Table I, where x_1 (theory) is set by the maximum of the Doppler or Voigt values as given above and compared with an accurately calculated x_1 (numerical) taken from the actual profiles ($\bar{L} = 0.01\ cm$).

Separate rate equations are now set-up for each transition describing the density of photons in the plasma,

$$\frac{dN_p^{\nu}}{dt} = N_j\, A_{ji} + \frac{1}{t_s}\, N_p^{\nu}\, \frac{N_j}{N_i} - \left\{\frac{1}{t_s} + \frac{1}{t_e}\right\} N_p^{\nu} \tag{11}$$

where j and i denote upper and lower states and A is the Einstein coefficient. The terms on the right hand side characterize, in order, the processes of spontaneous emission, stimulated emission, stimulated absorption, and escape from the plasma. Each rate equation for state densities will also be modified by the transport terms (where appropriate transitions occur) giving,

$$\frac{dN_i}{dt} = \sum_j W_{ji}\, N_j - \sum_j W_{ij}\, N_i + \frac{1}{t_s} N_p^{\nu} - \frac{1}{t_s}\, \frac{N_j}{N_i}\, N_p^{\nu} \tag{12}$$

where W represents the processes referred to in the previous section.

In practice equations 5 and 6 become undefined at small values of τ_o, hence, smooth interpolations were added to keep the transition from an optically thick to an optically thin line analytically defined.

This radiation transport model relies on the fact that the photon distribution from a given transiton will spread sufficiently into the wings to allow stabilization on a time scale short compared with plasma time scales of interest. This equilibration time is given by[11]

$$t_1 = (\tau_o - 1)\,\frac{\bar{L}}{\tau_o c} = \left(1 - \frac{1}{\tau_o}\right)\frac{\bar{L}}{c} \tag{13}$$

Since typical plasma lengths are less than 10^{-2} cm and time scales for the rate equations are $\sim 10^{-12}$ sec, t_1 is relatively smaller for even marginally thick lines. That is to say, as a line becomes thick enough to require a transport treatment, the line profile has *already* broadened sufficiently for equilibration to satisfy the above criteria.

The radiation calculation to determine the plasma emission is accomplished using three separate equations, one each for bremsstrahlung[12] (with unit Gaunt factor),

$$R_{brem} = 1.53 \times 10^{-38}\,\sqrt{T_e}\,N_e \sum_{Z,j} Z_j^2\,N_{Z,j}\,\frac{\mathrm{W}}{\mathrm{cm}^3} \tag{14}$$

radiative recombination,

$$R_{rr} = 1.6 \times 10^{-19}\,N_e \sum_{Z,j} N_{Z+1,0}\,\alpha_{Z+1,0;\,Z,j}\,\chi_{Z,j}\,\frac{\mathrm{W}}{\mathrm{cm}^3} \tag{15}$$

and line emission,

$$R_{line}^{(thin)} = 1.6 \times 10^{-19} \sum_{Z,i,j} \Delta E_{ij}\,A_{ij}\,N_{Z,i}\,\frac{\mathrm{W}}{\mathrm{cm}^3} \tag{16}$$

$$R_{line}^{(thick)} = 1.6 \times 10^{-19} \sum_{Z,\nu} \Delta E_{\nu}\,\frac{N_p^{\nu}}{t_e}\,\frac{\mathrm{W}}{\mathrm{cm}^3} \tag{17}$$

where α is the radiative recombination rate coefficient. The three contributions are then summed and inserted in the electron temperature equation as the term R.

III. PRELIMINARY INVESTIGATIONS

In preparation for the studies discussed in section II, we have used the code to shed light on some interesting preliminary problems as well as to compare our results with other similar but more detailed calculations. Some of these results will be presented in the following sections.

A. *Comparison of Rate Coefficients* — several methods have been used to calculate electron-ion collisional excitation rate coefficients as was mentioned in section II. Comparisons have been made between these methods for the purpose of weighing the inaccuracy introduced into the simulation by using more approximate (but relatively simpler) calculations for the rates. The first comparison studied the results of a distorted wave (DW) calculation, a semi-classical impact parameter (SCI) approximation, and a parameterized Born approximation (BORN) as applied to determine several collisional excitation rate coefficients of the heliumlike ion of aluminum. The BORN method was used to calculate rate coefficients from two different sets of parameters, one describing hydrogenic systems[10] and one for heliumlike species[13] (designated BORN(*H*) and BORN(*He*)). The results are depicted graphically in Figs. 6-14. The SCI method is shown only for allowed lines, since no simple semi-classical prescription is available for forbidden transitions. In addition, the BORN method is shown only for those transitions which were specifically parameterized by the authors[10,13] (hence, no $\Delta n = 0$ transitions for BORN(*H*) and only $n = 1$ to $n = 2$ and $n = 2$, $\Delta N = 0$ transitions for BORN(*He*)). Since we consider the DW calculation to be the most sophisticated of those considered here, we will use it as the standard of accuracy by which we make comparisons.

Consider, first, the SCI and DW calculations. For $\Delta n = 1$ transitions, the quantitative agreement appears somewhat good, however, qualitatively, the temperature dependence of the SCI rate coefficients is clearly incorrect at higher temperatures. The accuracy of the method deteriorates as the transition energy decreases; notice the poor agreement between the $3d - 4p$ and $2p - 3d$ transitions (Fig. 9) and the $\Delta n = 0$ transitions (Fig. 12). The agreement is reasonably accurate for transitions from the ground state for which $\Delta l = 1$. The accuracy of the SCI method is strongly dependent on the value of the oscillator strengths employed in the calculation. To obtain oscillator strengths for higher Z materials, we extrapolated many tabulated values from lower Z ions[4] and compared the results, quite favorably, with studies done by Lin *et al.*,[14] Schiff *et al.*,[15] Weiss,[16] and Smith and Wiese;[17] the results are shown for a few transitions in Figs. 15-18.

Definite trends are evident when the BORN(H) method is compared to the DW calculation quantitatively. For large energy separations the BORN(H) formula yields consistently lower values for the excitation rate by about 30%, as typified by the the Lyman transitions. This trend reverses itself for the smaller energy differences such as the Balmer and Paschen series, where the BORN(H) calculation gives typically greater values. The parameter constants, α and χ used in formula 4 were calculated for a hydrogenic system, however, and the agreement between these two methods is expected to improve with increasing Z as the heliumlike ion more closely resembles a single electron orbiting a highly-charged core.

Several rate coefficients were calculated using the BORN approximation but employing parameters fitted to heliumlike transitions;[13] the results have been plotted in Figs. 6,7,12,13,14 for a few transitions, including some involving change of spin. The $1s - 2s^1$ transition compares excellently with the DW rate, and the $1s - 2p^3$ also gives a favorably representation, but

the temperature dependence of the $1s - 2p^1$ transition is not accurate at higher temperatures (Fig. 7). In addition, the agreement between the two methods is very poor for the $2s^1 - 2p^1$, $2p^3 - 2s^1$, and $2p^3 - 2p^1$ transitions (Figs. 12 and 14), both quantitatively and, as seen in Fig. 14, qualitatively.

A second rate coefficient comparison was made between the BORN(H) and DW methods when applied to the hydrogenlike ion; also, the rates calculated independently using a Coulomb-Born approximation without exchange[10] were compared where possible to check agreement with our hydrogenlike aluminum rate coefficients. The DW and BORN calculations were checked for C VI as well as Al XIII to establish whether the accuracy of the BORN method was Z-dependent. In all cases calculated, the discrepancy between the three methods never exceeded 25% and was usually on the order of 5-10%, with slightly better (but not significant) accuracy obtained for the Al XIII ion.

B. *Validity of a Statistically Populated Hydrogenlike Ion* — in order to calculate level populations and radiation more economically, we have represented the hydrogenic ions in our model as a system of 'n' levels, as was stated in the previous section, rather than treat each nl level separately. This approximation assumes that the collisional coupling between different l sublevels of a given n level is sufficiently rapid that the sublevels relax to their statistical distributions on an instantaneous time scale relative to the other transition times populating the sublevels.

In order to verify this assumption we used the condition derived by Sampson[18] to determine the lowest n value at which the states should be statistically populated,

$$1.3 \times 10^{-16} \left(\frac{n}{Z}\right)^{8.5} T_e^{1/4} N_e \geq 1 \qquad (2 \leq Z \leq 10)$$

and

$$1.1 \times 10^{-15} \frac{n^{8.5}}{Z^8} N_e \geq 1 \qquad (11 \leq Z \leq 19) \tag{18}$$

with T_e in degrees kelvin. For a carbon plasma at 300 eV, an electron density of only $4.3 \times 10^{17}\ cm^{-3}$ is required for equilibration of the $n = 2$ levels, a density which is usually exceeded for plasmas of interest in this work. For aluminum and argon, the criterion yields 1×10^{21} and $1.8 \times 10^{22}\ cm^{-3}$ for $n = 2$, and 3.4×10^{19} and $5.6 \times 10^{20}\ cm^{-3}$ for $n = 3$, respectively. The condition for statistical equilibrium is met easily for the $n = 3$ levels by both plasmas, since our study is concerned with plasmas of ion density $5 \times 10^{19}\ cm^{-3}$ and greater. However, the $n = 2$ levels are marginally *unequilibrated*, according to condition (18), and should actually be treated as separate levels. The criterion may be relaxed somewhat due to the fact that it is derived for a plasma which is optically thin, whereas in reality, radiation trapping due to opacity in plasmas at these densities should drive the level populations closer to their LTE values. In particular, the ($2s$, $2p$) level system of the hydrogenlike ion may not be statistically equilibrated due to the depletion by strong radiative decay of the $2p$ state. In an optically thick plasma, however, photo-excitation will exceed collisional excitation as the dominant mechanism populating this state, preferentially increasing its density compared to the $2s$ level and restoring, to a degree, the statistical equilibrium of the $n = 2$ level. Since the L_α line is consistently optically thick for the plasma densities considered in this study, we have chosen to represent the $n = 2$ level as a single degenerate state as we have done with the $n \geq 3$ levels.

C. *Degeneracy of levels of the heliumlike ion* — the structure of the heliumlike ion differs from that of the hydrogenlike ion in that (i) two distinct spin systems (ortho- and parahelium) are present, and (ii) the energy differences between the l components of an n level are larger, particularly at low n values. This would seem to indicate that a similar attempt to model only "degenerate" n levels of the heliumlike ion by assuming that the various l components of both

spin systems equilibrate instantaneously to their statistical populations would yield incorrect results. However, as principal quantum number increases, the energy separation between l sublevels of each spin system may decrease sufficiently that, once again, ion-ion collisions may be the dominant transition mechanism causing population changes among these levels. Moreover, it is well known that resonance transitions occurring in the singlet system of the heliumlike ion tend to be optically thick for dense plasmas, due to the persistently high concentration of the ground state of this closed-shell configuration over a wide temperature range. Hence, as was stated in the previous section, opacity effects should optically pump some of the lower depleted levels, restoring their populations and driving them closer to their statistical distributions.

In order to quantitatively assess these effects on the excited level populations of the heliumlike ion and to detemine at what value of n, the l levels relax to their statistical populations, we calculated the ion-ion collision rates coupling the nl components for the $n = 2, 3$ levels of the argon heliumlike ion and compared them with the fastest radiative rates depleting their population densities. To calculate the rate coefficient for collisional excitation by ions we used a formula by Drawin[19] with a guillotine factor given by Weisheit[20],

$$X_{ij}^{ion} = \left(\frac{\mu}{M_e}\right)^{1/2} Z^2 \, X_{ij}^{elec} \left[1 + \left(\frac{T_e}{\Delta E}\right)^2\right] \left[\left(\frac{\mu}{M_e}\right)^2 + \left(\frac{T_e}{\Delta E}\right)^2\right]^{-1} \frac{cm^3}{sec} \tag{19}$$

where μ is the reduced mass of the incident and target ion and Z is the charge of the incident ion. For the $n = 2$ level, the fastest radiative rate was for the $(1s - 2p^1)$ transition, $1.07 \times 10^{14}\ sec^{-1}$, while the combined electron and ion excitation rate coupling the $2s^1$ to the $2p^1$ state was $2.3 \times 10^{11}\ sec^{-1}$ at $T_e = 1.5$ keV and $N_e = 10^{21}\ cm^{-3}$. Clearly, the $2p^1$ level will be depleted so rapidly by spontaneous decay that equilibration with the $2s^1$ will never occur at these plasma parameters. It is also very unlikely that opacity effects will repopulate the $2p^1$

level sufficiently to overcome the 3-orders-of-magnitude difference between these two rates. The $2s^3 - 2p^3$ collisional excitation rate is basically identical to the singlet transition (the electron-ion rate is larger but the ion-ion rate is smaller), but the radiative decay rate of the $2p^3$ state is only $6.07 \times 10^{11}\ sec^{-1}$. For the assumption of statistical equilibration to be valid, one should expect that the collisional rate should exceed the radiative rate by at least a factor of *ten*. Although the rates are close, opacity effects should be small for the intercombination line, due to the small Einstein A value, hence these levels should not equilibrate at the assumed plasma parameters either.

Repeating the calculation for the $n = 3$ level, we find that the collision rate for the $(3s^1 - 3d^1)$ transition will *equal* the fastest radiative decay rate $(2p^1 - 3d^1)$ at $Ne = 7.7 \times 10^{20}\ cm^{-3}$ and the same condition occurs for the $(3d^1 - 3p^1)$ collisional rate and the $(1s - 3p^1)$ radiative decay at $N_e = 6 \times 10^{20}\ cm^{-3}$ (level energies were taken from Ermolaev and Jones[21]). At $N_e \simeq 10^{21}\ cm^{-3}$, conditions for statistical equilibration of the $n = 3$ level are marginally satisfied, but even small opacity effects should have an influence on the repopulation of radiatively depleted l levels. An approximate measure of this effect is the ratio of the photo-excitation to the collisional excitation rate for one of these states. We can express this ratio, based on our frequency diffusion transport model, as

$$\frac{\Psi_{ij}}{X_{ij}} = \frac{\gamma(1 - p_q)}{1 + p_q\gamma} \tag{20}$$

where $\gamma = \tau_o\ (\pi \ln t_o)^{1/2}$ and p_q is the quenching parameter defined by $p_q = Y/(A + Y)$, with A being the Einstein A of the line and Y the rate accounting for all other processess which deplete the level, excepting A. Typical values of these quantities at the plasma conditions previously quoted are $p_q \sim 0.3$ and $\tau_o \sim 15$ (for a 100 micron plasma), yielding a ratio of 2.17 for the $(1s^1 - 3p^1)$ transition. Hence, doubling the rate at which the ground state populates the

$3p^1$ state should have a significantly beneficial effect on equilibrating the $n = 3$ singlet levels. The triplet system for this level should parallel the singlet system for the same reasons which were stated in the discussion of the $n = 2$ system.

In view of the above study, we have chosen to include the four individual nl components in our model for the $n = 2$ level system, hence, taking explicit account of all processes coupling each of the four states. However based on our discussion of the $n = 3$ level we expect that collisions will dominate the higher states, sufficiently aided by pumping due to radiation trapping, and we have chosen to describe all higher levels ($n \geq 3$) of the argon heliumlike ion as two degenerate n states, a singlet and a triplet. In the argon model used in our preliminary investigations, however, we have omitted the $n = 3, 4$, and 5 triplet states as an initial approximation.

D. *Comparison with a Similar Model* — We have compared the results predicted by our model with that of a similar calculation[22] designed for implementation in cylindrical geometry calculations. However, by analyzing calculations of the atomic state of the plasma in the optically thin approximation, meaningful comparisons can be made between the two models. Both simulations were at constant ion density of $5 \times 10^{19}\ cm^{-3}$ and electron temperature of 550 eV for an aluminum plasma. The only differences in the two calculations were in the structure of the K-shell excited levels, and some relevant conclusions have resulted from this study.

The heliumlike level system was nearly identical in both models, with the exception that the $5p^1$ level was missing in our calculation (see Fig. 1). The populations of the included states are shown in Table II for both simulations. The differences between the densities are less than 15% in all cases except the $1s2p^3$ level where the error is 37%. This is attributable to the fact

that slightly different decay rates were used for the ($1s - 2p^3$) transition[23] in the two models. The consistency of both calculations, however, is clearly evident.

Contrasting differences are noticeable in the results obtained for the hydrogenlike ion. Our model contained a degenerate system of the lowest $3n$ levels, with each l component assumed to be populated statistically (see last section), while the other calculation included only p states up to the $4p^1$ level. In addition, no collisional coupling processes were included between these p levels. The densities shown in the table for p states from our model are obtained from the n-level densities by simple degeneracy ratios. Significant differences are seen to occur between the two models, becoming larger as the principal quantum number increases. We attribute this trend in the differences to the progressively smaller fraction of the total n population occupying the p state as n increases above 2, indicating the necessity for including a more comprehensive level structure for the lower n values.

E. *Comparison of Optically Thick and Thin Calculations* — To see the profound effect of radiation trapping on the calculation, two separate runs modeling a laser-heated plasma were made with identical input parameters, changing only the transport calculation from perfectly thin to thick. The results presented are for a 77 micron radius sphere of aluminum plasma at a density of 7.6×10^{19} ions/cm^3. The laser pulse was 0.2 nsec (FWHM) and a total of 0.8 Joules of laser energy were absorbed in the sphere. Electron temperatures peaked along with the laser pulse at about 430 eV and decayed slowly to about 110 eV. The line spectra for the thick case are shown in Figs. 19 and 20, with solid horizontal bars indicating the emission in the thin case. In general, the optically thick lines will decrease and thin ones will increase when radiation is trapped. The L_α and L_β lines of Al XII are seen to decrease since they are thick, while all other Al XII lines increase due to the enhanced population from the upper levels of the thick

transitions causing greater overall excited state populations. However, all of the Al XIII lines are seen to increase over the thin case, even though the L_α line is marginally reabsorbed ($\tau_o(MAX) \approx 6$). The apparent increase is due predominantly to the pumping of the Al XIII ground state by collisional ionization of the Al XII excited states, now with increased populations. The Al XIII ground state now couples to its excited states in turn, increasing their populations. To verify this, another run was made, ("thick-thin") with the heliumlike lines transported but the hydrogenlike lines untransported. The results are shown on the graphs by the dotted horizontal lines on the Al XIII lines (Al XII line emission was, as expected, unchanged). Note the increase in the $H(L_\alpha)$ line in the "thick-thin" case over the thin case and then another decrease as both ions are calculated as thick; the result, therefore, is a net *increase* in the emission of this line even though it is somewhat thick.

The effect of photon-pumping on the upper levels of thick lines has a profound effect on the thin-line emission; order of magnitude increases are seen to occur in $H(L_\alpha)$, H_α, H_β, He_α and He_β line emission corresponding to similar increases in the upper states of these transitions. The heliumlike intercombination line also displays some enhancement since the $2p^3$ state is strongly collisionally coupled to the pumped $2p^1$ state at these electron densities. It is hoped that some of the more dramatic "thickness" effects discussed here might be exploited for diagnostic purposes to determine spatially resolved parameters in these plasmas.

IV. DISCUSSION

In an attempt to shed some light on a few of the more subtle problems that exist in the mathematical modeling of the atomic state of high-temperature, high-density plasmas, we have been able to reach some significant conclusions based on our investigations. In addition, the results obtained thus far will guide our future attempts to model atomic structure and its radia-

tive effects on the energy balance of these plasmas, and therefore, in summary, a disussion of these results is fruitful.

The acquisition of reliable rate coefficients, in particular, those describing collisional excitation and de-excitation, have always presented a major obstacle to those who would include ionization dynamics in their plasma models. Many of the scattering methods are too detailed and involve expensive computer codes to generate rates which are calculated with more accuracy than the plasma model may initially demand. Other simpler calculations may not give a comprehensive treatment of all rates of a given ionization stage, or are based on assumptions which introduce intolerable or, more often, unknown inaccuracies into the rates. In view of our preliminary results in this area, we feel several conclusive statements can be made. The well-known semi-classical impact parameter formula can be used to generate rates for dipole allowed transitions with varying degrees of error. For most resonance transitions of the heliumlike system the oscillator strengths have already saturated at medium Z to near their hydrogenic values, and can be obtained by extrapolation techniques to good accuracy, thereby yielding rates accurate to about 10%, with our standard of comparison being set by a reliable distorted-wave-with-exchange calculation. For transitions of lower energy difference, this method becomes unreliable, yielding large quantitative differences along with a more deviant temperature dependence. The values generated for transitions in which $\Delta n = 0$ may be as much as an order of magnitude in error, making this a totally unacceptable method for this case. In addition, the method is undefined for forbidden transitions. A simple hydrogenic Born approximation, on the other hand, yields rates for *all* transitions within a heliumlike spin system, and they tend to agree favorably with the temperature dependence of the more accurate DW rates. The error is larger for resonance transitions than it is with the SCI calculation but yields better agreement for other higher level transitions.

Specific parameters developed for heliumlike ions were also calculated in the Born approximation and found to give very inconsistent results. Rates for some transitions differed by less than 10% from the DW calculation while others showed discrepancies of an order of magnitude or more with a totally dissimilar temperature dependence from that predicted by the distorted wave calculation.

However, encouraged by the excellent agreement between the BORN and DW calculations for several transitions, it is conceivable that a complete set of collisional rates could be calculated for heliumlike ions using the BORN formula, equation (18), if a more appropriate and comprehensive set of α and χ parameters could be determined, and that these parameter fits would compare quite favorably with the rates calculated using more accurate but more detailed scattering theories.

Although we have sought to investigate simple methods of generating an approximate set of rate coefficients for use in a general K-shell structural model, we do not wish to underemphasize the value or accuracy of a distorted wave calculation, specifically for $\Delta n = 0$ and spin-flip transitions, nor the importance of its use in benchmarking any attempt at an empirically determined parameter-fit of rate coefficients as we have done here.

In the case of the hydrogenlike ion, we have established that the Born approximation yields excellent agreement with a DW treatment of collisional excitation rates, and that the agreement improves with increasing Z, yielding a simple and economical method of obtaining a complete set of accurate values. In addition, we have shown that under certain plasma conditions, little or no accuracy is lost in employing a single level representation for the various l states of a given n level for this ion, since ion-ion collisions at high densities insure that individual nl sublevels will equilibrate to their statistically weighted densities on very short time scales

(up to some n_{max}, that is where $\Delta E_{nn'}$ becomes small and $\Delta n = 1$ transitions become as likely; then the statistical population among the l-sublevels is re-distributed). A study was also made to determine whether this simplifying approach to the level modeling could be applied to heliumlike ions. It was found, also, that ion-ion collisions and opacity effects in dense plasmas at high-temperature can successfully re-distribute the populations of levels having principal quantum number greater than 2, such that the l sub-levels of an n level are maintained at their statistically weighted densities and can mathematically be represented as a single degenerate level. The importance of the environmental effects of the plasma on this value of n, however, should be re-emphasized, and any plasma environment differing significantly from the one considered here must be re-assessed.

A phenomenological radiation transport scheme has been implemented in our plasma radiation model to partially account for the effects of self-absorption on population densities and subsequent radiation emission. An attempt to compare this model with a spherical ray-trace calculation[24] is underway to hopefully provide a means of assessing the capability of our frequency diffusion transport as well as to improve it.

"Thin plasma" comparisons between this model and a similar rate equation scheme have resulted in some interesting conclusions concerning the completeness of an atomic structural model for a given ion. Good agreement was obtained between the two calculations for population densities of the heliumlike ion (where level structure was similar), usually within 15%. However, for the hydrogenlike ion, only p states were modeled in the other simulation, whereas a complete set of levels up to $n = 4$ was included in our calculation. In addition, no collisional coupling was included between the p states of the other model. The discrepancy in the predicted values for populations of these excited levels in the two calculations can be as much

as a factor of 2. Hence, we conclude that omission of the neighboring s, d, and f angular momentum levels from a structural model may result in a significant loss of accuracy in excited state populations due to collisional and radiative coupling to these missing states. Moreover, we find as was substantiated by Fig. 20, that in failing to include these levels, a serious loss of radiation is incurred in the calculation which results from inter-level radiative transitions between states greater than $n = 1$ and for which $\Delta n \neq 0$, $\Delta l = 1$. Our simulation, as shown in this graph, predicts significant radiation from these transitions, enhanced by the reabsorption of the resonant line radiation.

Comparisons of calculations between optically thick and optically thin plasmas have demonstrated some profound effects of reabsorption on the population densities (of ground states as well as excited states) and the line emission from optically thick plasmas. These comparisons have shown that the optical pumping of excited levels due to trapped radiation and subsequent strong collisional coupling upward can cause dramatic increases in population densities of higher level excited states. This well-known effect of opacity on the radiation can result in enhancement of thin line emission often by as much as an order of magnitude or more, as shown in Figs. 19 and 20 (see specifically the He_α, He_β and $He(2p-3d)$ lines).

In addition, we have demonstrated that the increased populations of the excited states of ion Z due to this optical pumping can cause a similar increase in the ground state population of the $Z + 1$ ion through the collisional ionization process. This, in turn, can cause increases in populations of the excited states of the $Z + 1$ ion to the extent that this increase may result in such a significant enhancement of the radiation from these levels that it will overshadow any decrease (relative to the thin case) one would expect due to the thickness of the line. The startling result, therefore, is that an optically *thick* line may emit *more* radiation than it would if it

were calculated in the optically *thin* approximation, as does the $H(L_\alpha)$ line in Fig. 19. The neglect of this possible enhancement could have a decidedly detrimental effect on the diagnostic interpretation of spectral line emission from dense laser-heated plasmas and the plasma parameters which are inferred from their ratios.

ACKNOWLEDGEMENT

This work was supported in part by the Defense Nuclear Agency.

REFERENCES

1. K. G. Whitney and J. Davis, JAP *45*, 5294 (1974).

2. S. I. Braginskii, *Reviews of Plasma Physics*, edited by M. A. Leontovich (Consultants Bureau, New York, 1965).

3. L. Spitzer, Jr., *Physics of Fully Ionized Gases*, 2nd ed. (Interscience, New York, 1962).

4. W. Wiese, M. Smith, and B. Miles, *Atomic Transition Probabilities*, NBS Publ. No. 22, Vol. II.

5. H. Van Regemorter, Aph. J. **136**, 906 (1962).

6. C.W. Allen, *Astrophysical Quantities*, 2nd ed. (Athlone Press, University of London, London, 1965).

7. J. Davis, JQSRT *14*, 549 (1974).

8. J. Davis, P. C. Kepple, and M. Blaha, NRL Memorandum Report 2939 (1974).

9. L. A. Vainshtein, I. I. Sobel'man, Lebedev Report No. 66 (1967), and I. I. Sobel'man, *Introduction to the Theory of Atomic Spectra*, Pergamon Press, Oxford, 1972.

10. R. K. Landshoff and J. D. Perez, Phys. Rev. A *13*, 1619 (1976).

11. P. S. Julienne and J. Davis, NRL Memorandum Report 2556 (1973).

12. H. R. Griem, *Plasma Spectroscopy* (McGraw-Hill, New York, 1964).

13. L. A. Vainshtein and V. P. Shevel'ko, Preprint No. 26 (in Russian), Lebedev Physics Institute, Academy of Sciences of the USSR, Moscow (1974); see also, A. V. Vinogradov, I. Yu. Skobelev, and E. A. Yukov, Sov. J. Quant. Electron., *5*, 630 (1975).

14. C. D. Lin, W. R. Johnson, and A. Dalgarno, Aph. J. *217*, 1011 (1977).

15. B. Schiff, C. L. Pekeris, and Y. Accad, Phys. Rev. A *4*, 885 (1971).

16. A. W. Weiss, J. Res. NBS *71A*, 163 (1967).

17. M. W. Smith and W. L. Wiese, Aph. J. Supp. No. 196, *23*, 103 (1971).

18. D. H. Sampson, J. Phys. B: Atom Molec. Phys. *10*, 749 (1977).

19. H. W. Drawin, Z. Physik, *225*, 483 (1969).

20. J. C. Weisheit, J. Phys. B: Atom. Molec. Phys., Vol. 8, No. 15, 2556 (1975).

21. A. M. Ermolaev and M. Jones, J. Phys. B: Atom. Molec. Phys, *7*, 199 (1974).

22. P. Kepple, J. Davis, J. Apruzese, and V. Jacobs, Bull. APS *22*, No. 9, 1107 (1977).

23. C. D. Lin, W. R. Johnson, and A. Dalgarno, Phys. Rev. A, *15*, 154 (1977).

24. J. P. Apruzese, J. Davis, and K. G. Whitney, JAP *48*, 667 (1977).

Table I — Values of x_1 for various lines over a range of electron temperatures. (The analytic value is above the numerical value.)

N_i / T_e	$He(L_\alpha)$		$He(L_\beta)$		$He(L_\alpha)$	
	10^{19}	7×10^{19}	10^{19}	7×10^{19}	10^{19}	7×10^{19}
50eV	3.1	8.2	2.2	2.42	2.2	4.2
	3.3	8.0	2.2	2.6	2.3	4.0
100	2.3	5.8	2.1	2.35	2.1	2.75
	2.6	5.6	2.1	2.35	2.1	2.9
300	2.2	3.5	1.96	2.2	2.0	2.5
	2.2	3.35	1.96	2.2	2.0	2.6
500	2.1	2.6	1.88	2.18	1.95	2.45
	2.1	2.8	1.88	2.18	1.95	2.5
1000	2.0	2.5	1.76	2.1	1.9	2.3
	2.0	2.6	1.76	2.1	1.9	2.3

Table II — Comparison of state population densities (Given in ions/cm^3).

State		Our Model	Kepple et al
Al XII	$1s^2$	3.72×10^{19}	3.53×10^{19}
	$1s2p^3$	2.86×10^{17}	4.59×10^{17}
	$1s2p^1$	2.80×10^{15}	2.67×10^{15}
	$1s3p^1$	1.09×10^{15}	1.00×10^{15}
	$1s4p^1$	7.50×10^{14}	6.40×10^{14}
Al XIII	$1s$	1.14×10^{19}	1.90×10^{19}
	$2p$	1.35×10^{15}	8.60×10^{14}
	$3p$	2.93×10^{14}	5.68×10^{14}
	$4p$	1.78×10^{14}	3.97×10^{14}
Al XIV		8.16×10^{17}	3.21×10^{17}

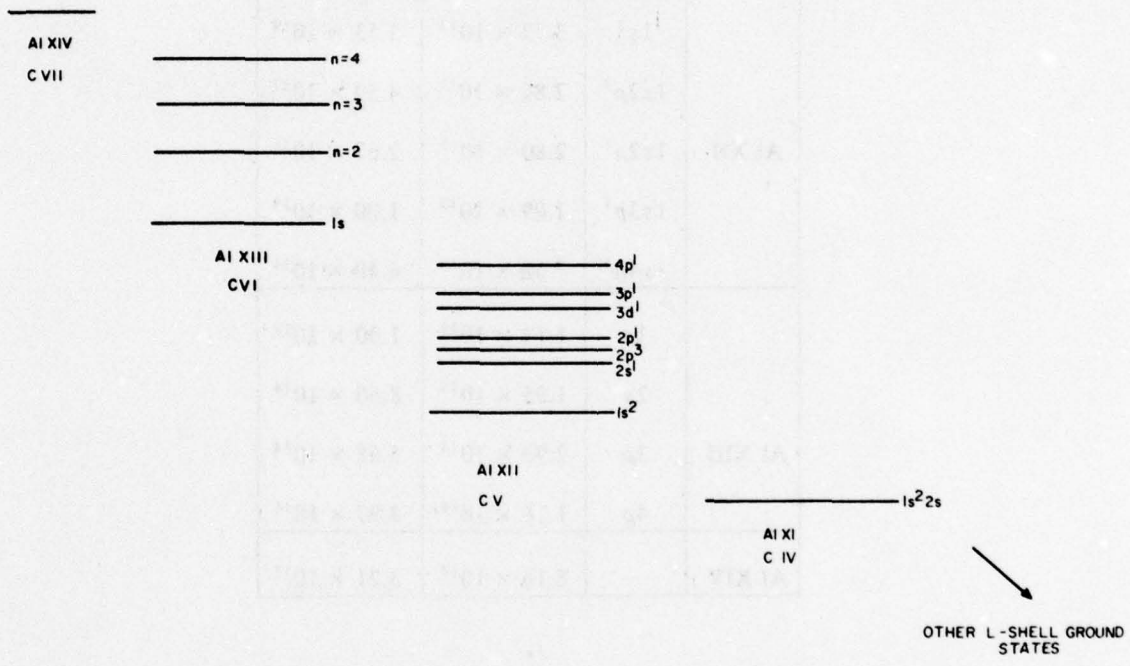

Figure 1 — Carbon and aluminum energy level diagram.

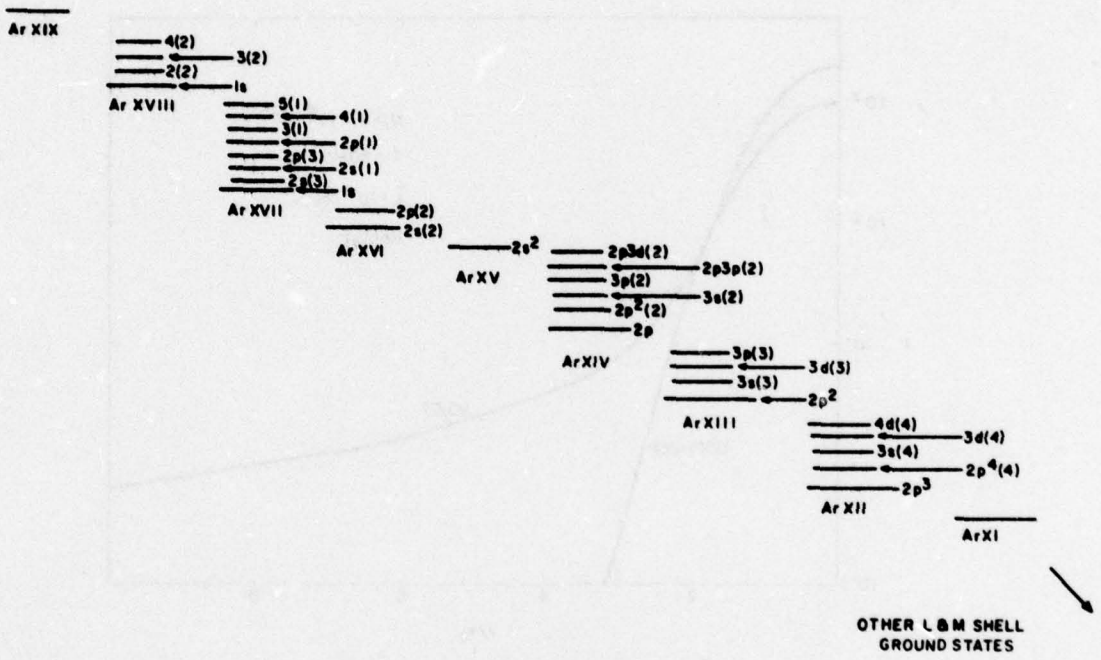

Figure 2 — Argon energy level diagram

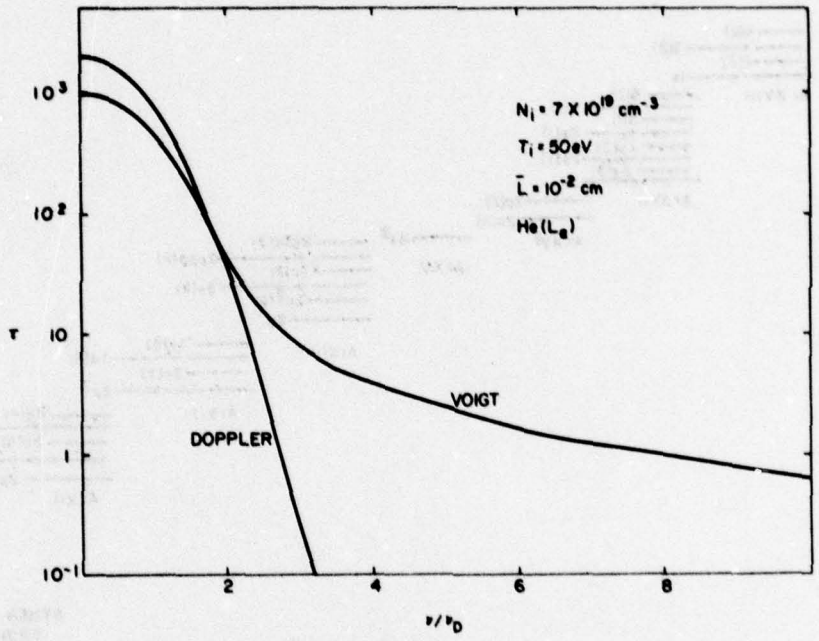

Figure 3 — Heliumlike (L_α) line profiles — aluminum.

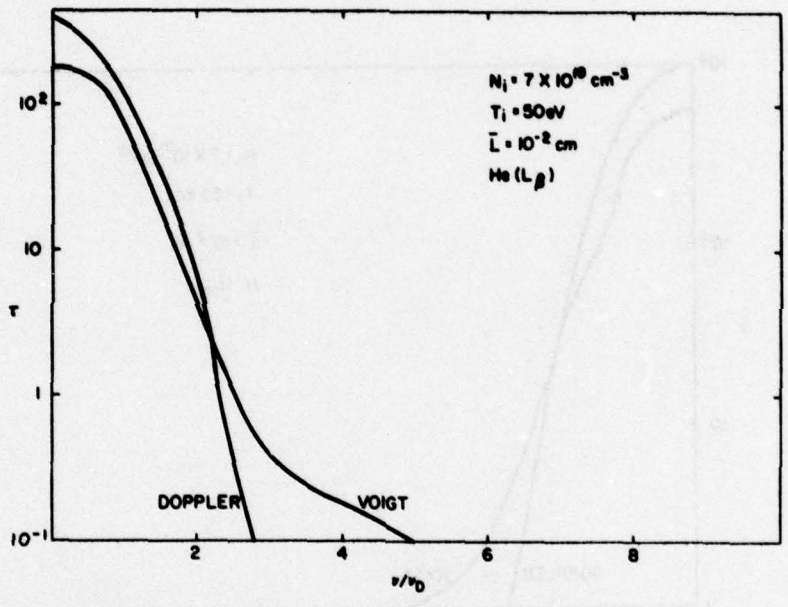

Figure 4 — Heliumlike (L_β) line profiles — aluminum.

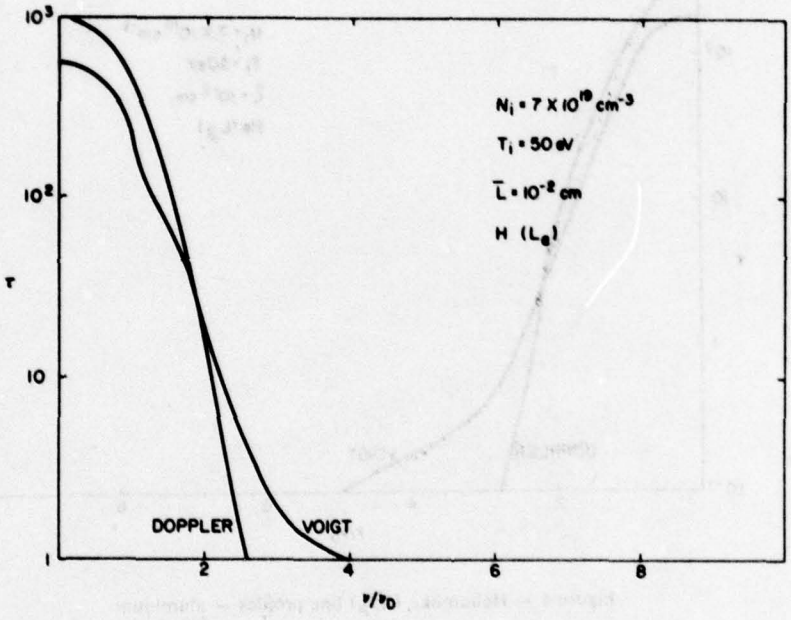

Figure 5 — Hydrogenlike (L_α) line profiles —aluminum.

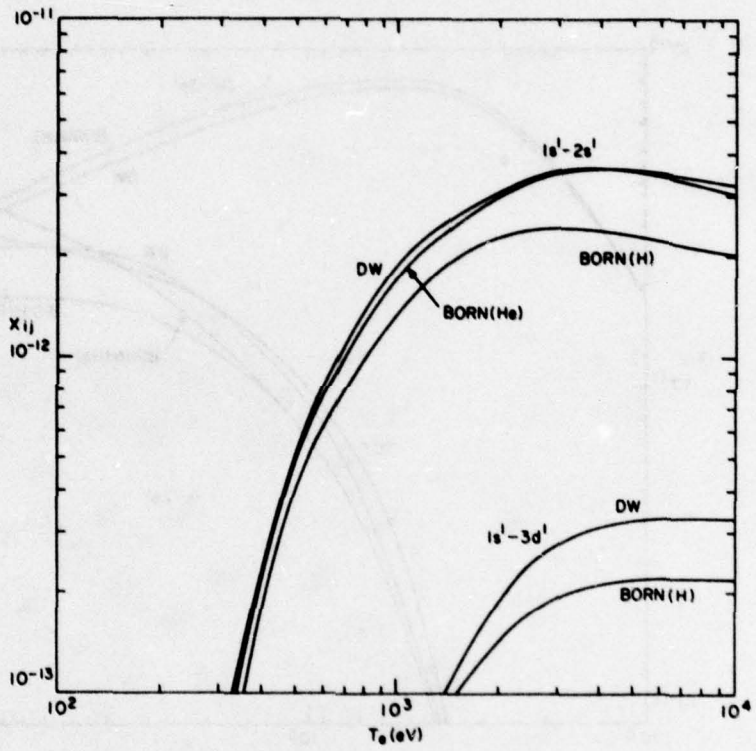

Figure 6 — Electron collisional excitation rate coefficients for heliumlike aluminum transitions.

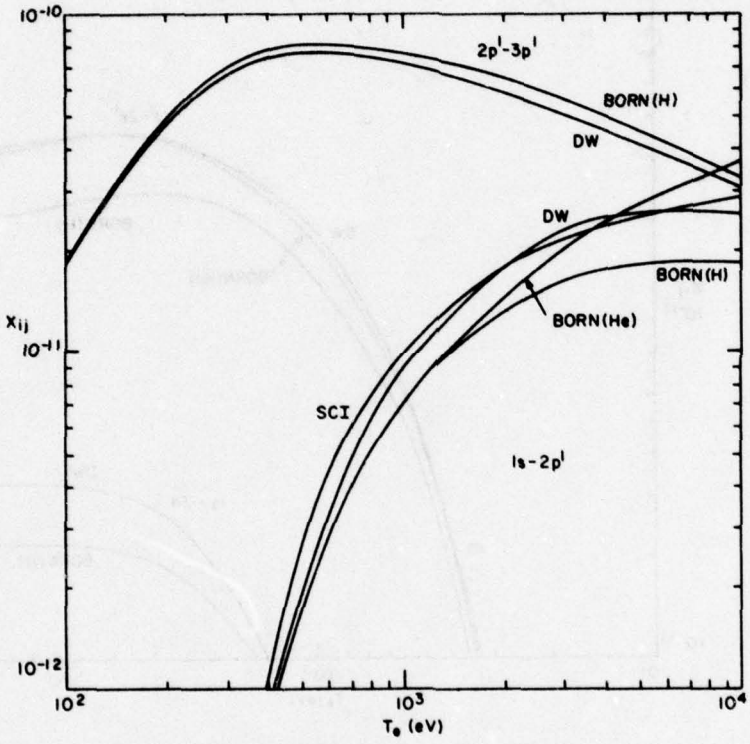

Figure 7 — Electron collisional excitation rate coefficients for heliumlike aluminum transitions.

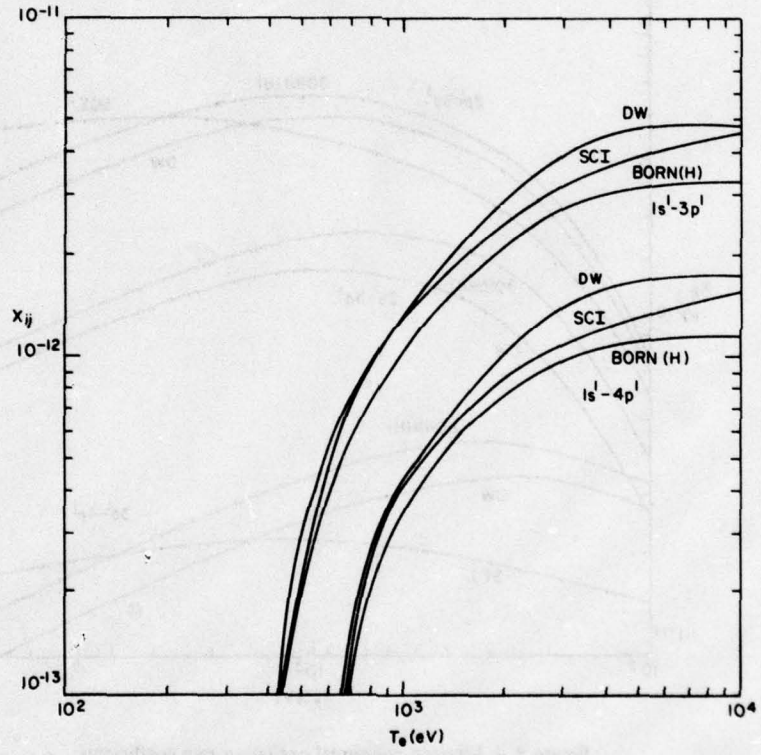

Figure 8 — Electron collisional excitation rate coefficients for heliumlike aluminum transitions.

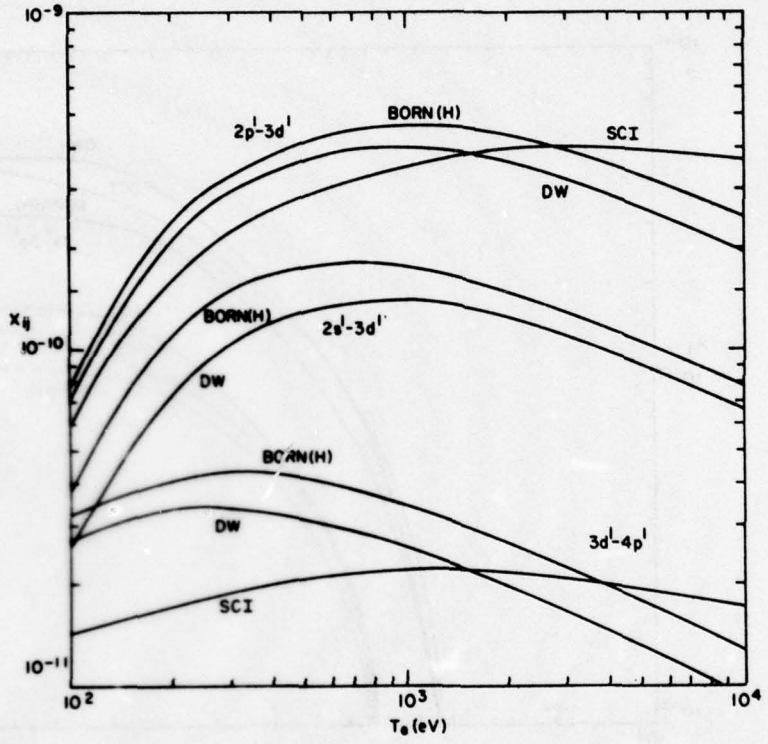

Figure 9 — Electron collisional excitation rate coefficients for heliumlike aluminum transitions.

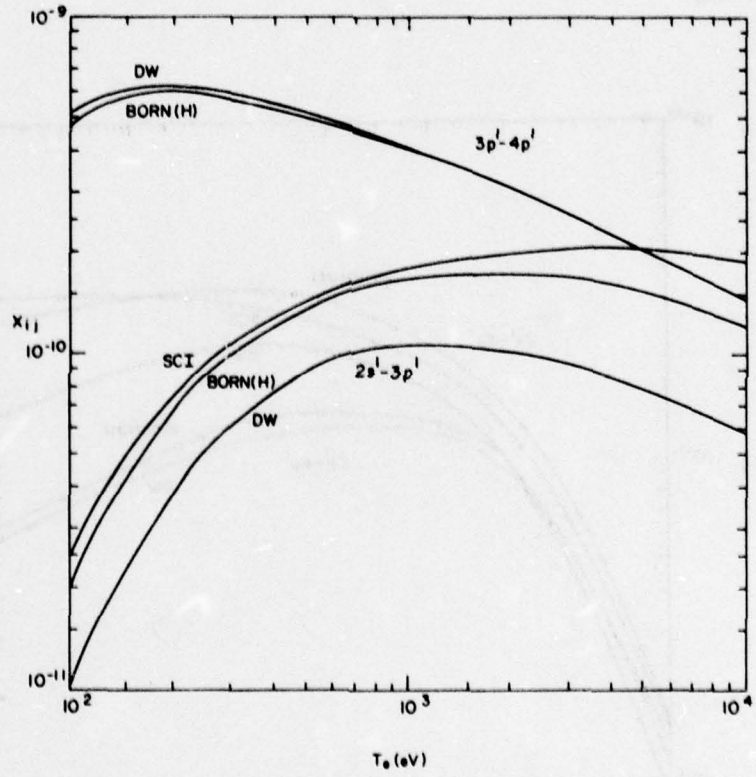

Figure 10 — Electron collisional excitation rate coefficients for heliumlike aluminum transitions.

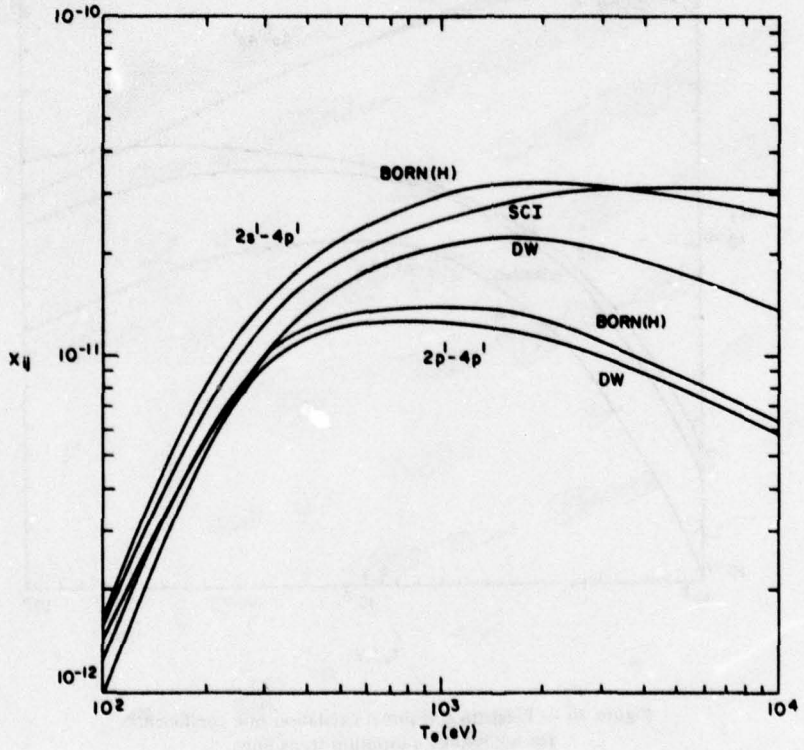

Figure 11 — Electron collisional excitation rate coefficients for heliumlike aluminum transitions.

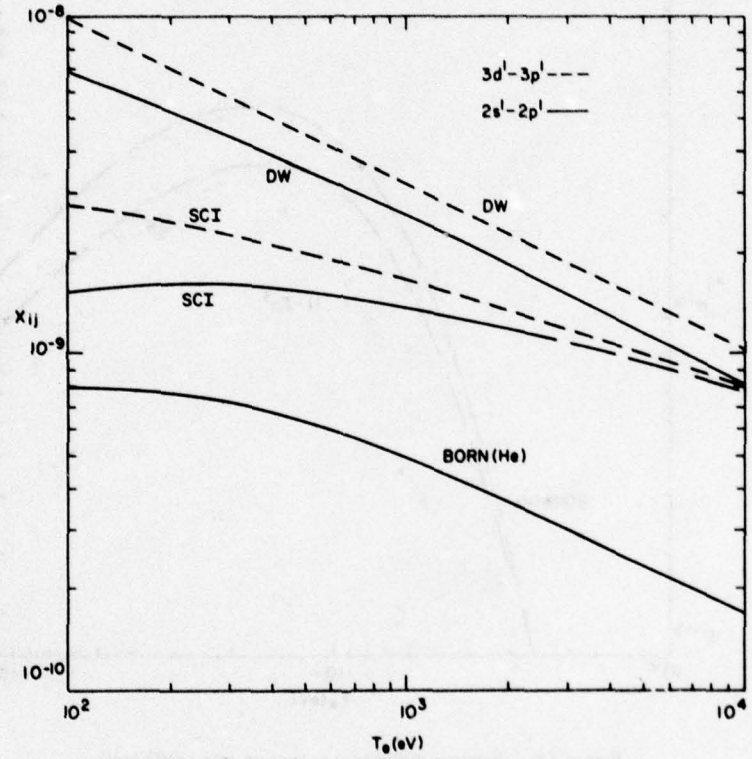

Figure 12 — Electron collisional excitation rate coefficients for heliumlike aluminum transitions.

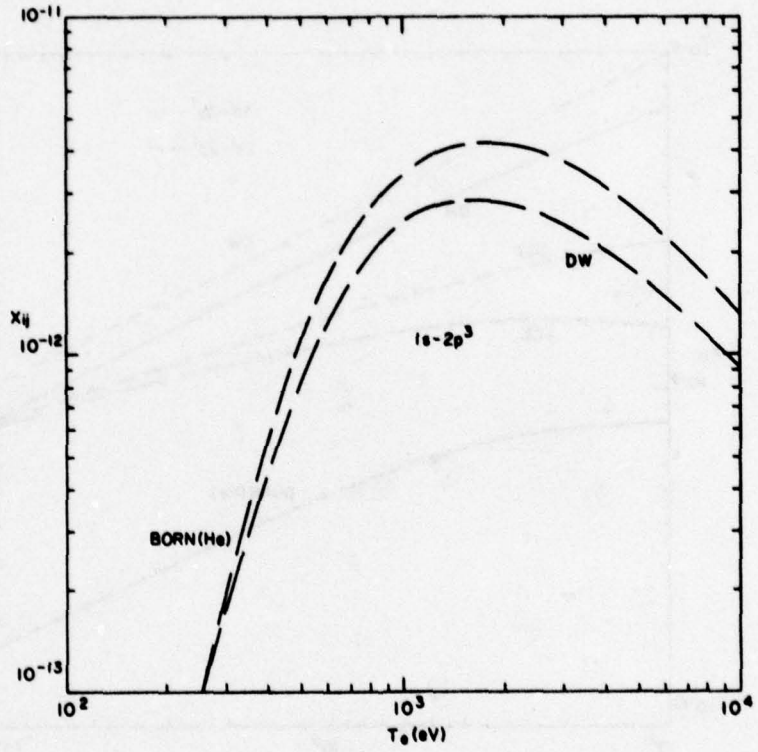

Figure 13 — Electron collisional excitation rate coefficients for heliumlike aluminum transitions.

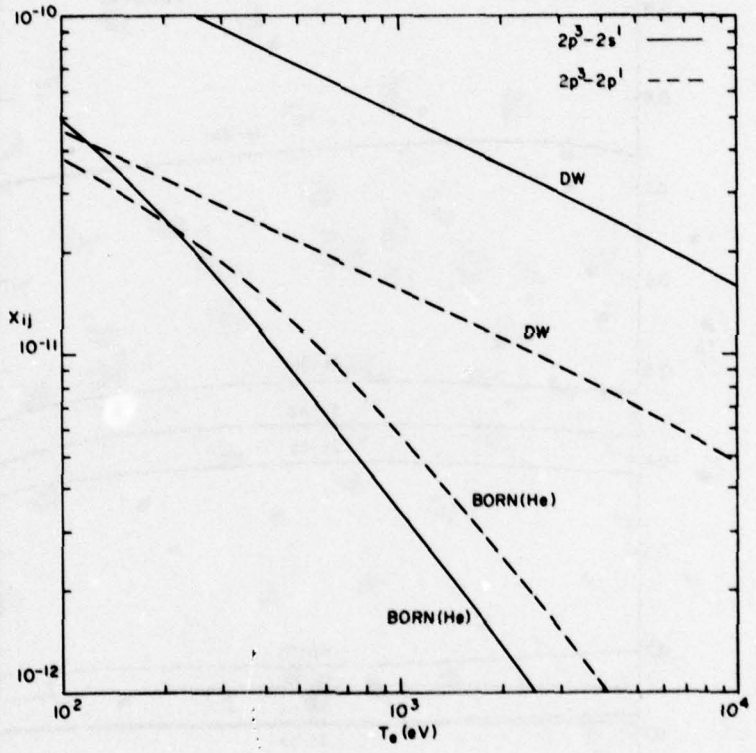

Figure 14 — Electron collisional excitation rate coefficients for heliumlike aluminum transitions.

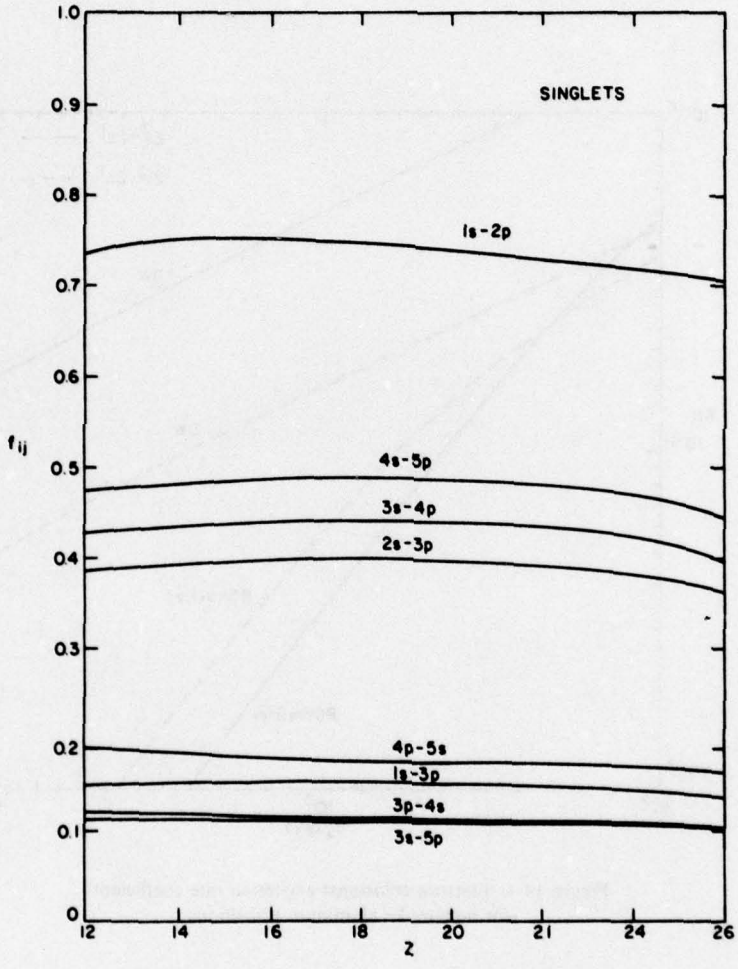

Figure 15 — Singlet transition oscillator strengths for heliumlike ions.

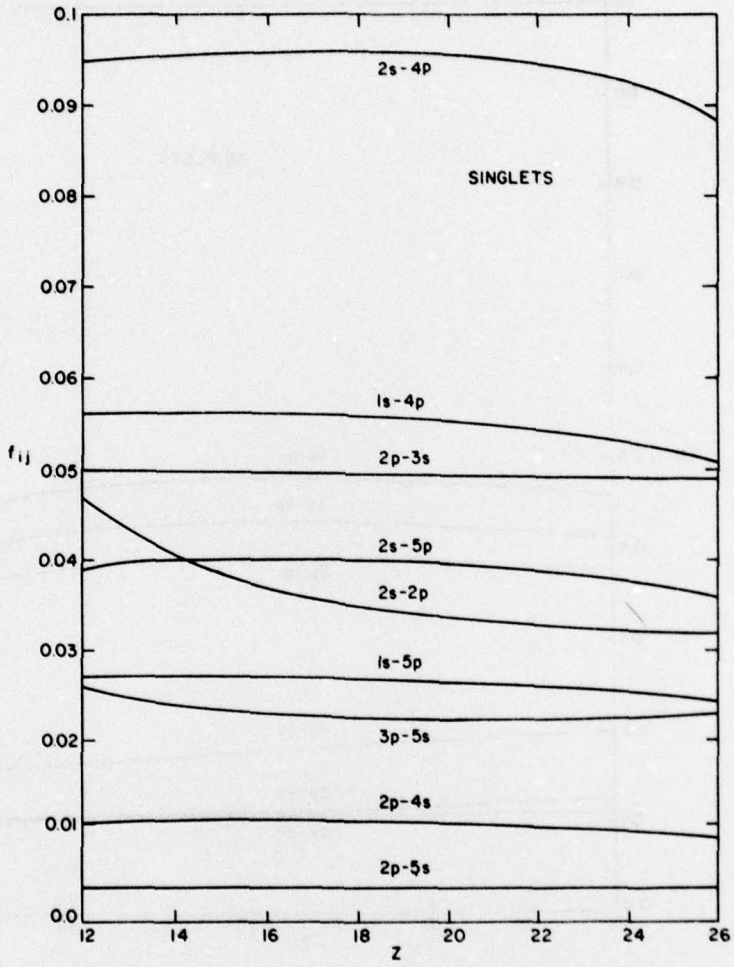

Figure 16 — Singlet transition oscillator strengths for heliumlike ions.

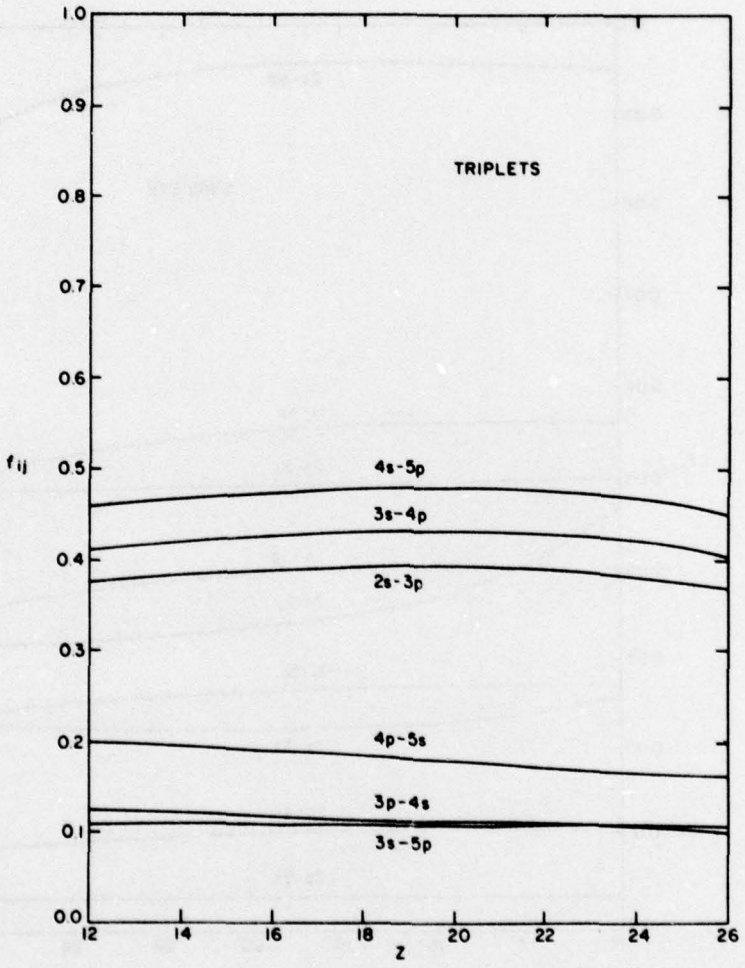

Figure 17 — Triplet transition oscillator strengths for heliumlike ions.

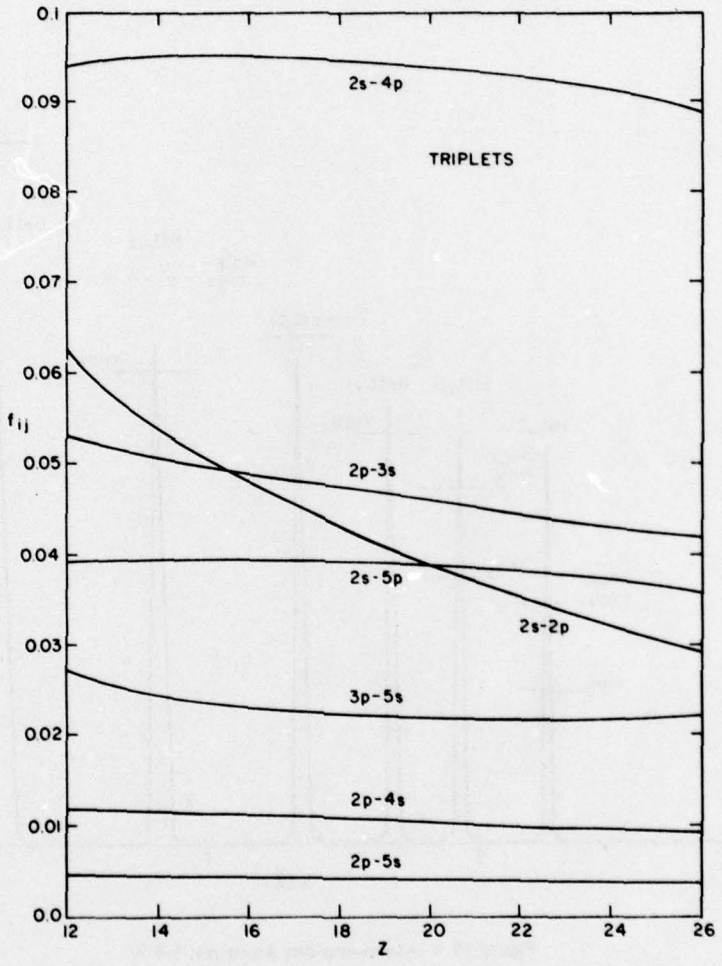

Figure 18 — Triplet transition oscillator strengths for heliumlike ions.

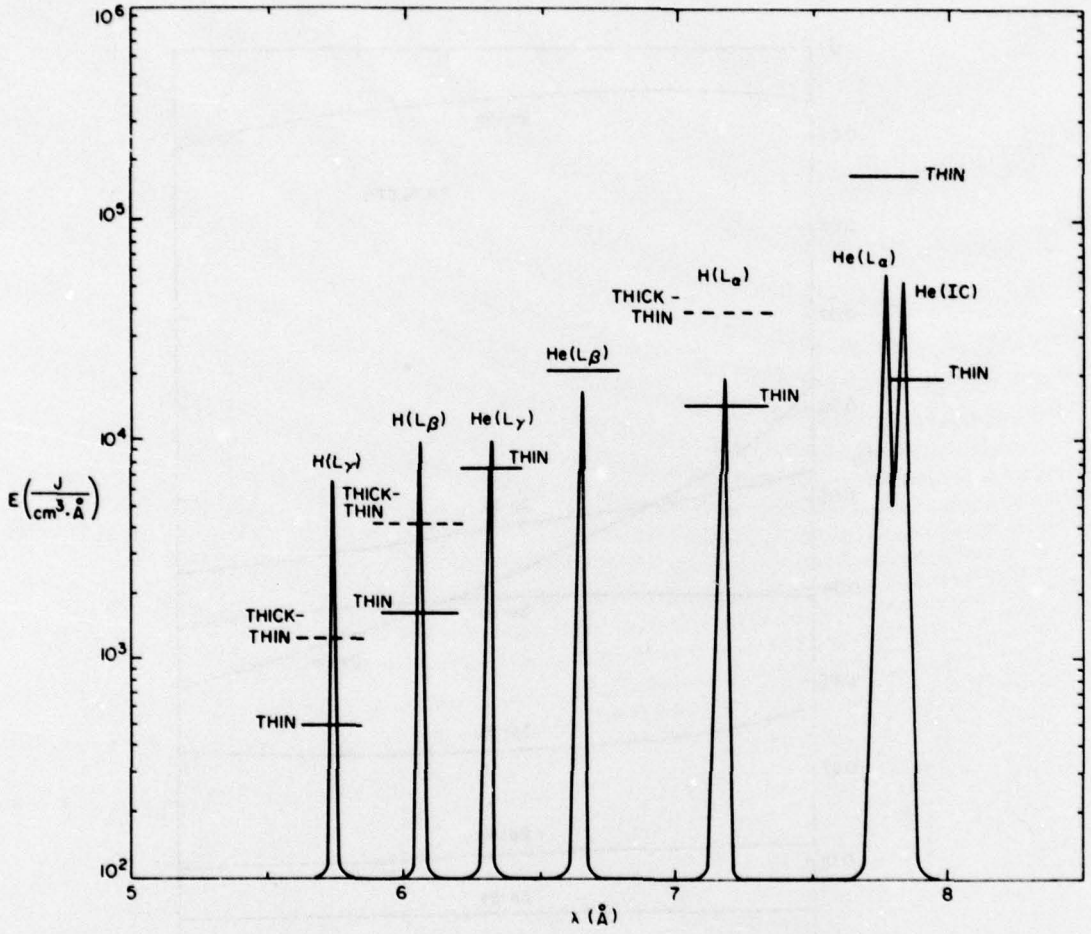

Figure 19 — Aluminum line spectrum; 5-8 Å

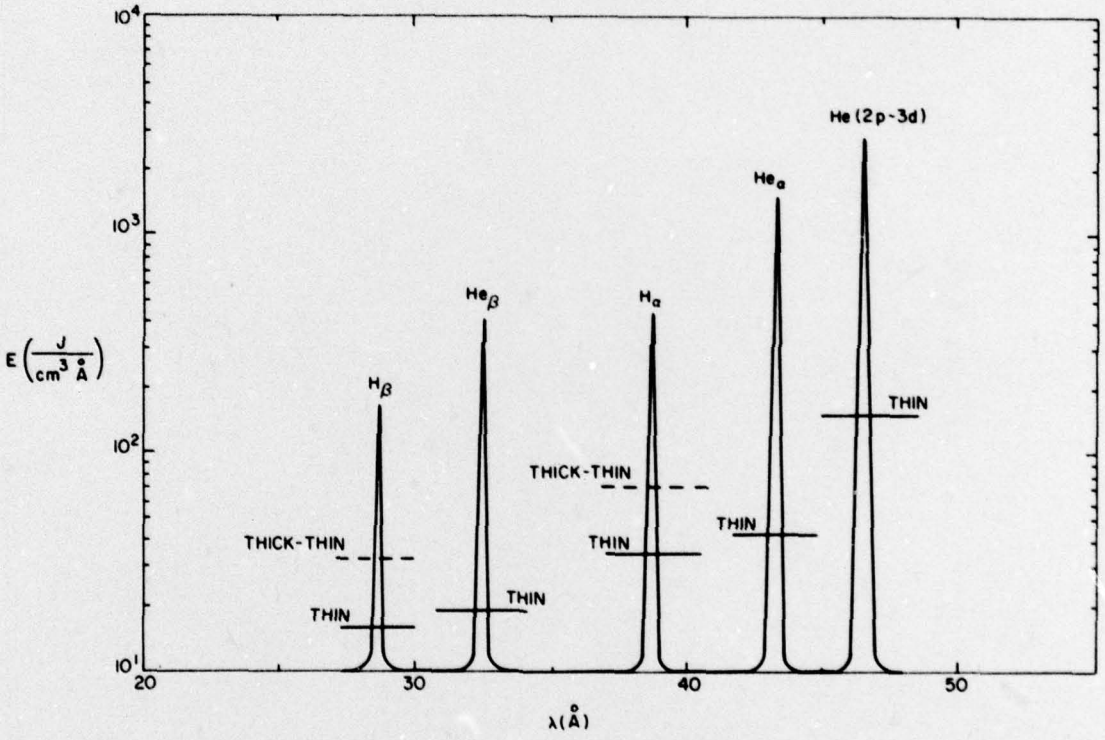

Figure 20 — Aluminum line spectrum; 20-50 Å

DISTRIBUTION LIST

1. Assistant to the Secretary of Defense
   Atomic Energy
   Department of Defense
   Washington, D.C. 20301

   Attn: ATSD (AE)

2. Defense Documentation Center
   Cameron Station
   Alexandria, Virginia 22314

   (12 copies if open publication, otherwise 2 copies)

   Attn: TC

3. Director
   Defense Intelligence Agency
   Washington, D.C. 20301

   Attn: DTICI Robert I. Rubenstein

4. Director
   Defense Nuclear Agency
   Washington, D.C. 20305

   Attn: STVL
   Attn: TISI
   Attn: TITL ------ 3 copies
   Attn: RAEV

5. Commander
   Field Command
   Defense Nuclear Agency
   Kirtland Airforce Base, New Mexico 87115

   Attn: FCPR

6. Director
   Joint Strat TGT Planning Staff
   Offutt Airforce Base
   Omaha, Nebraska 68113

   Attn: JSAS

7. Chief
Livermore Division Field Command DNA
Lawrence Livermore Laboratory
P.O. Box 808
Livermore, California 94550

Attn: FCPRL

8. Under Secretary of Defense
for RSCH and FNGRG
Department of Defense
Washington, D.C. 20301

Attn: S&SS (OS)

9. Commander
BMD System Command
P.O. Box 1500
Huntsville, Alabama 35807

Attn: SSC-TEN

10. Deputy Chief of Staff for
RSCH DEV and ACQ
Department of the Army
Washington, D.C. 20310

Attn: DAMA-CSM-N

11. Commander
Harry Diamond Laboratories
2800 Powder Mill Road
Adelphi, Maryland 20783

Attn: DELHD-RBH
Attn: DELHD-NP
Attn: DELHD-RCC John A. Rosado
Attn: DELHD-RBH Paul A. Caldwell
Attn: DELHD-TI Tech. Library

12. Commander
U.S. Army Nuclear and Chemical Agency
7500 Backlick Road
Building 2073
Springfield, Virginia 22150

Attn: Library

13. Commander
U.S. Army Test and Evaluation Command
Aberdeen Proving Ground, Maryland 21005

Attn: DRSTE-EL

14. Chief of Naval Operations
Navy Department
Washington, D.C. 20350

Attn: Robert A. Blatse 604C4

15. Commander
Naval Electronic Systems Command
Naval Electronic Systems CMD HQS
Washington, D.C. 20360

Attn: Code 5032

16. Commanding Officer
Naval Intelligence Support Center
4301 Suitland Road, Bldg. 5
Washington, D.C. 20390

Attn: NISC-45

17. Officer-In-Charge
Naval Surface Weapons Center
White Oak, Silver Spring, Maryland 20910

Attn: Code WR43
Attn: Code WA501 Navy Nuc Progms Office

18. Commander
Naval Weapons Center
China Lake, California 93555

Attn: Code 533 Tech Lib.

19. Ion Physics Corporation
South Redford Street
Burlington, Massachusetts

Attn: H. Milde

20. IRT Corporation
P.O. Box 81087
San Diego, California 92138

Attn: R. Mertz

21. JAYCOR
1401 Camino Del Mar
Del Mar, California 92014

Attn: F. Wenaas

22. JAYCOR
205 S. Whiting Street
Suite 500
Alexandria, Virginia 22304

Attn: R. Sullivan

23. Kaman Sciences Corporation
P. O. Box 7463
Colorado Springs, Colorado 80933

Attn: A. Bridges
Attn: J. Hoffman
Attn: D. Bryce
Attn: W. Ware

25. Lockheed Missiles and Space Co., Inc.
3251 Hanover Street
Palo Alto, California 94304

Attn: Lloyd F. Chase

26. Maxwell Laboratories, Inc.
9244 Balboa Avenue
San Diego, California 92123

Attn: A. Richard Miller
Attn: Peter Korn
Attn: Alan C. Kolb

27. McDonnell Douglas Corporation
5301 Bolsa Avenue
Huntington Beach, California 92647

Attn: Stanley Schneider

28. Mission Research Corporation
735 State Street
Santa Barbara, California 93101

Attn: William C. Hart
Attn: C. Longmire

29. Mission Research Corp. - San Diego
P.O. Box 1209
La Jolla, California 92038

Attn: Victor A. J. Van Lint

30. Northrop Corporation (desires only 1 copy of CNWDI Material)
Northrop Research and Technology Center
3401 West Broadway
Hawthorne, California 90250

Attn: Library

31. Northrop Corporation
Electronic Division
2301 West 120th Street
Hawthorne, California 90250

Attn: Vincent R. Demartino

32. Physics International Company
2700 Merced Street
San Leandro, California 94577

Attn: DOC CON for Charles H. Stallings
Attn: DOC CON for Philip W. Spence

33. Pulsar Associates, Inc.
11491 Sorrento Valley Blvd.
San Diego, California 92121

Attn: Carleton H. Jones, Jr.

34. R and D Associates
P. O. Box 9695
Marina Del Rey, California 90291

Attn: C. MacDonald
Attn: George Fisher

35. Science Applications, Inc.
P. O. Box 2351
La Jolla, California 92038

Attn: J. Robert Beyster

36. Spire Corporation
P. O. Box D
Bedford, Massachusetts 01730

Attn: Roger G. Little

37. SRI International
333 Ravenswood Avenue
Menlo Park, California 94025

Attn: Setsud Dairiki

38. Systems Science and Software, Inc.
P. O. Box 1620
La Jolla, California 92038

Attn: Andrew R. Wilson

39. Texas Tech. University
P.O. Box 5404 North College Station
Lubbock, Texas 79417

Attn: Travis L. Simpson

40. TRW Defense and Space Systems Group
One Space Park
Redondo Beach, California 90278

Attn: Tech. Info. Center/S-1930

41. Vought Corp. (formerly LTV Aerospace Corporation)
Michigan Division
38111 Van Dyke Road
Sterling Heights, Michigan 48077

Attn: Tech. Lib.

42. Ford Aerospace and Communications Corp.
Ford and Jamboree Roads
Newport Beach, California 92663

Attn: Tech. Information Section

43. Ford Aerospace and Communications Corp.
3939 Fabian Way
Palo Alto, California 94303

Attn: D. McMorrow MS G30
Attn: Library

44. General Electric Company
Space Division
Valley Forge Space Center
P.O. Box 8555
Philadelphia, Pa. 19101

Attn: J. Peden VFSC, 4230M

45. General Electric Company - Tempo
Center for Advanced Studies
816 State Street
P.O. Drawer QQ
Santa Barbara, California 93102

Attn: DASIAC

46. Institute for Defense Analyses
400 Army-Navy Drive
Arlington, Virginia 22202

Attn: TDA Librarian R. Smith

47. AVCO Research and Systems Group
201 Lowell Street
Wilmington, Massachusetts 01887

Attn: Research Lib. A830 Rm 7201

48. BDM Corporation
7915 Jones Branch Drive
McLean, Virginia 22101

Attn: Technical Library

49. Boeing Company
P.O. Box 3707
Seattle, Washington 98124

Attn: Aerospace Library

50. Dikewood Industries, Inc.
1009 Bradbury Drive, S.E.
Albuquerque, New Mexico 87106

Attn: L. Davis

51. EG&G Washington Analytical Services Center, Inc.
P.O. Box 10218
Albuquerque, New Mexico 87114

Attn: Technical Library

52. University of California
Lawrence Livermore Laboratory
P.O. Box 808
Livermore, California 94550

Attn: L-18
Attn: L-153
Attn: John Nickolls A Div L-545 (Class L-33)
Attn: Tech. Information Dept L-3

53. Sandia Laboratories
P.O. Box 5800
Albuquerque, New Mexico 87115

Attn: DOC CON for 3141 Sandia Rpt. Coll.
Attn: DOC CON for 5240 Gerald Yonas

54. Samso/SK
Post Office Box 92960
Worldway Postal Center
Los Angeles, California 90009

(Space Comm. Systems)
Attn: SKF Peter H. Stadier

55. AF Weapons Laboratory, AFSC
Kirtland AFB, New Mexico 87117

Attn: CA
Attn: ELC
Attn: NT
Attn: SUL
Attn: DYP

56. Headquarters USAF/RD
Washington, D.C. 20330

Attn: RDQSM

57. Samso/Dy
Post Office Box 92960
Worldway Postal Center
Los Angeles, California 90009

Attn: DYS (Technology)

58. Samso/IN
Post Office Box 92960
Worldway Postal Center
Los Angeles, California 90009

Attn: Ind Maj Darryl S. Muskin
(Intelligence)

59. Samso/MN
Norton AFB, California 92409

Attn: MNNH
(Minuteman)